Supporting information:

Unraveling the impact of different thermal quenching routes on the luminescence efficiency of the $Y_3Al_5O_{12}$:Ce^{3+} phosphor for white light emitting diodes

Yuan-Chih Lin[1], Marco Bettinelli[2], Suchinder K. Sharma[1], Britta Redlich[3], Adolfo Speghini[4] and Maths Karlsson[1,*]

[1]*Department of Chemistry and Chemical Engineering, Chalmers University of Technology, SE-412 96 Göteborg, Sweden. E-mail: maths.karlsson@chalmers.se (Maths Karlsson);* [2]*Luminescent Materials Laboratory, Department of Biotechnology, University of Verona and INSTM, UdR Verona, 37134 Verona, Italy;* [3]*Radboud University, Institute for Molecules and Materials, FELIX Laboratory, Nijmegen, The Netherlands.* [4]*Nanomaterials Research Group, Department of Biotechnology, University of Verona and INSTM, UdR Verona, Strada Le Grazie 15, 37134 Verona, Italy.*

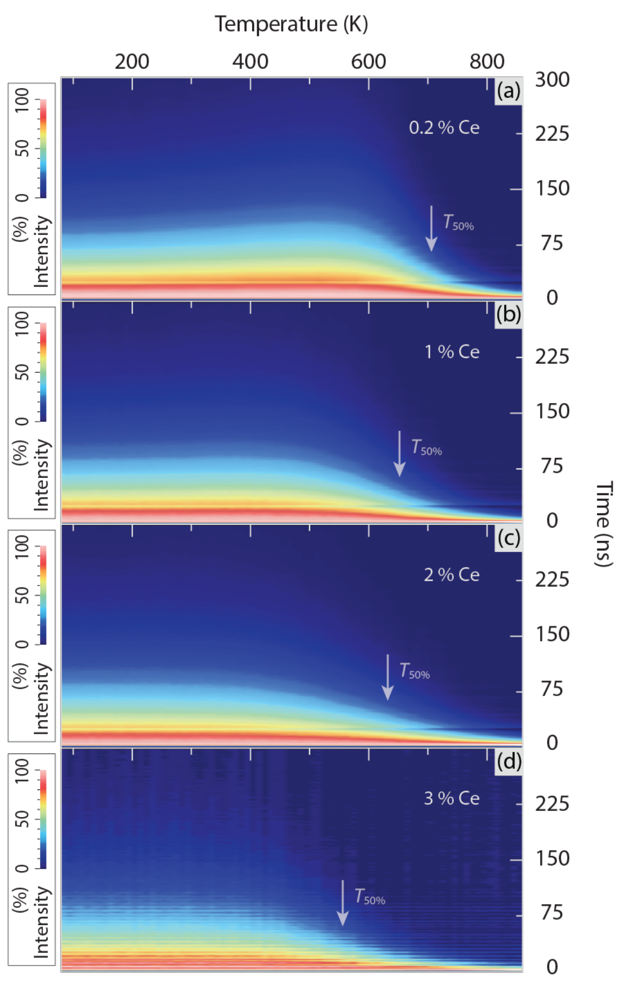

Figure S1 Luminescence decay curves of YAG:x%Ce^{3+} with x = (a) 0.2, (b) 1, (c) 2 and (d) 3, as a function of increasing temperature from 80 K to 860 K. $T_{50\%}$ is indicated by an arrow.

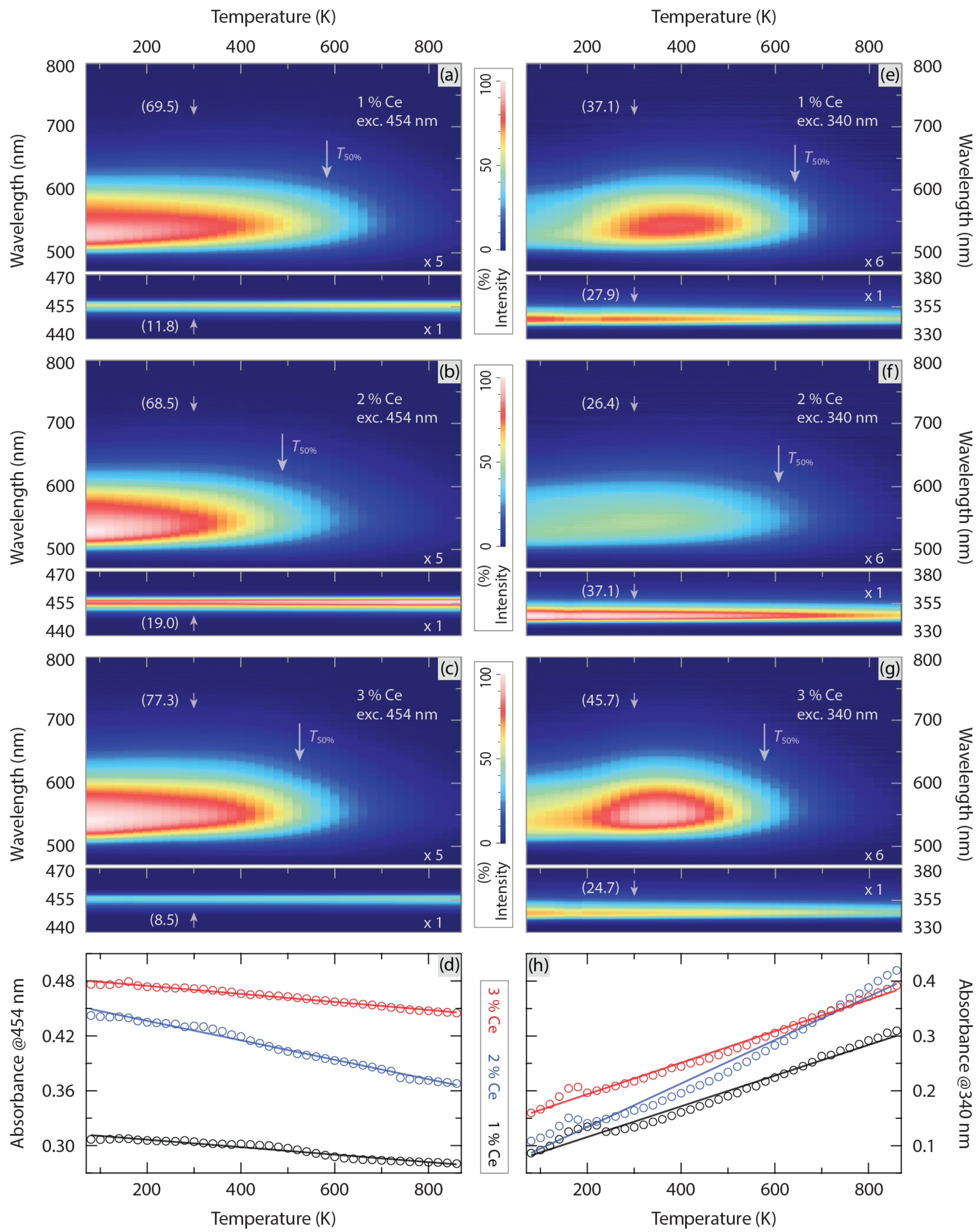

Figure S2 Spectra of emitted light from YAG:x%Ce^{3+} and reflected light of the excitation source (wavelength at 454 nm or 340 nm) in the temperature range of 80–860 K, where (a) $x = 1$, (b) 2 and (c) 3, upon excitation at 454 nm, and (e) $x = 1$, (f) 2 and (g) 3, upon excitation at 340 nm. Note that, to have a clear view, the intensity of the spectrum of emitted light (YAG:x%Ce^{3+}) is scaled by 5 times for excitation at 454 nm, and by 6 times for excitation at 340 nm. The integrated intensity of the spectrum of emitted light (YAG:x%Ce^{3+}), or reflected light (excitation source), at 300 K is shown in parentheses, with respect to that of the excitation source (= 100). $T_{50\%}$ is indicated by an arrow. (d,h) Absorbance of YAG:x%Ce^{3+} ($x = 1$, 2 and 3) at (d) 454 nm and (h) 340 nm, in the temperature range of 80–860 K.

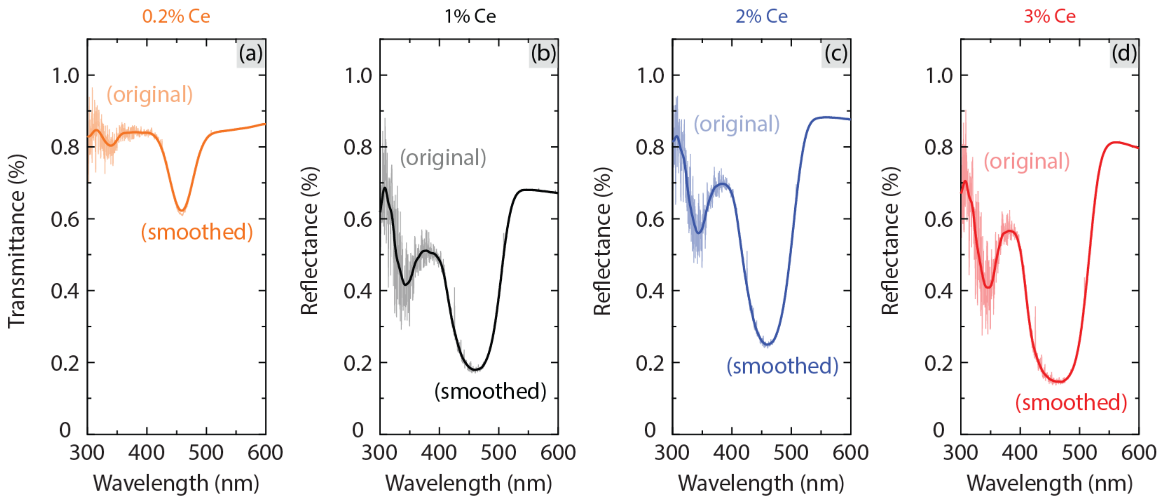

Figure S3 Original data of RT transmittance/diffuse reflectance spectra of YAG:x%Ce^{3+} with x = (a) 0.2, (b) 1, (c) 2 and (d) 3, before being smoothed and vertically offset.

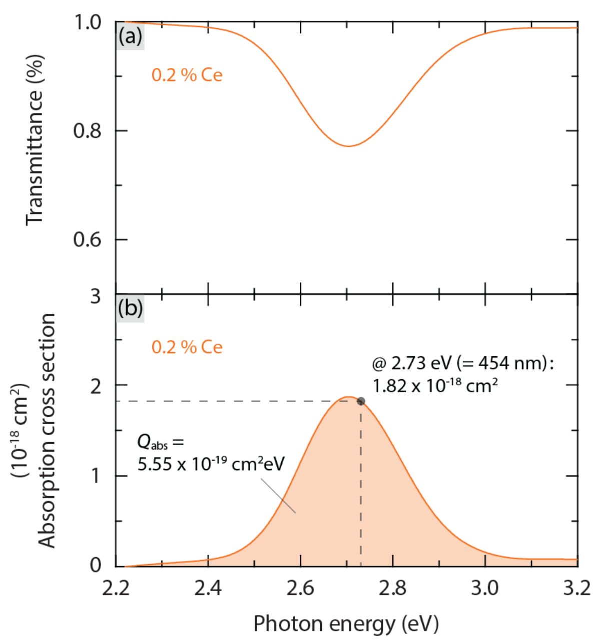

Figure S4 (a) RT transmittance spectrum of YAG:0.2%Ce^{3+}, *i.e.* the spectral data shown in Figure S3(a) with the background subtracted. (b) Absorption cross section of YAG:0.2%Ce^{3+}, converted from the spectrum in (a) using sample parameters such as thickness (= 50 μm) and density (= 4.56 mg/mm^3) for the single crystal film (YAG:0.2%Ce^{3+}).

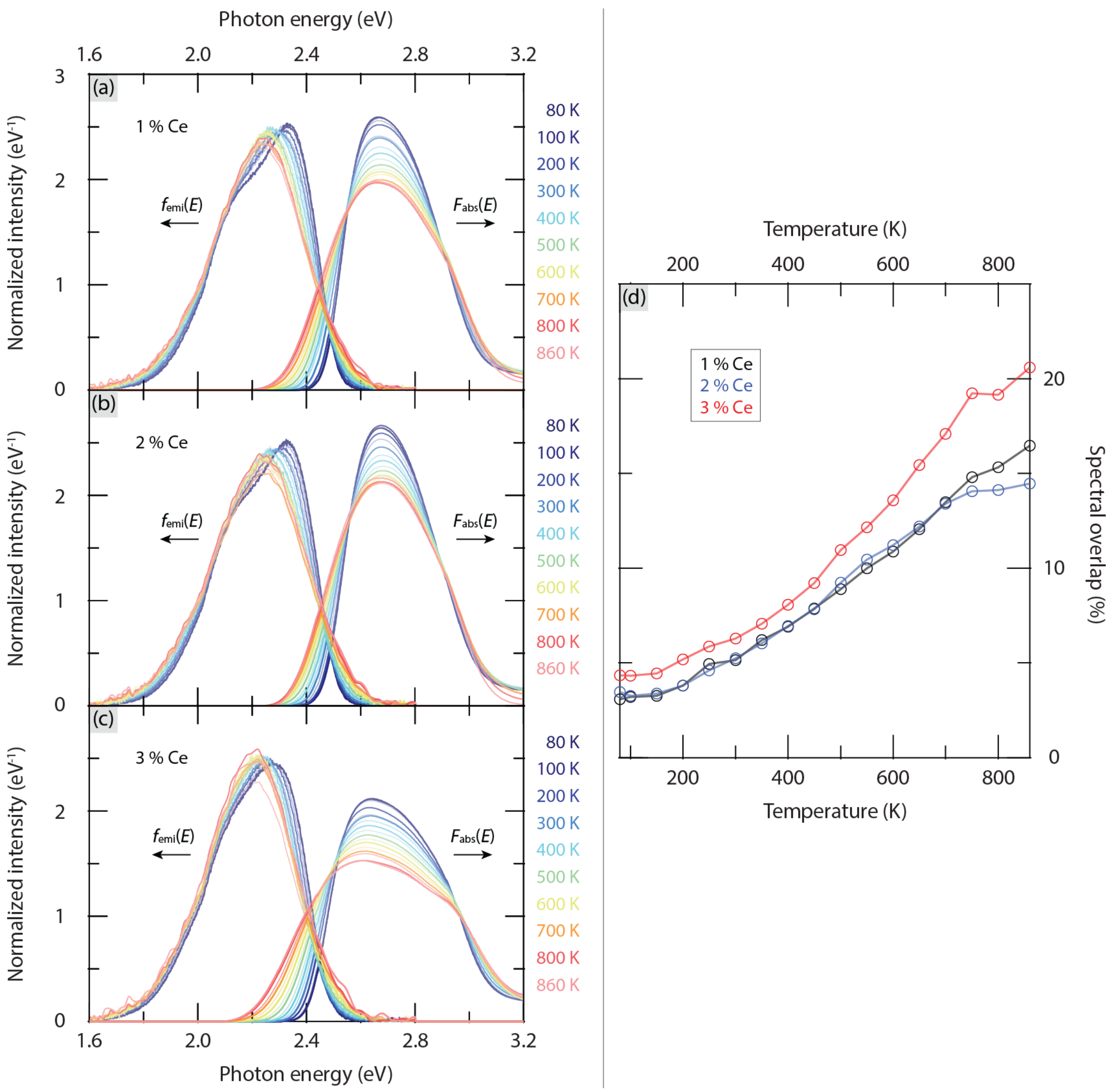

Figure S5 Normalized absorption and emission spectra of YAG:x%Ce^{3+} [denoted as $F_{abs}(E)$ and $f_{emi}(E)$, respectively, where E is the photon energy] in the temperature range of 80–860 K, where x = (a) 1, (b) 2 and (c) 3. (d) Spectral overlap for YAG:x%Ce^{3+} (x = 1, 2 and 3) as a function of increasing temperature from 80 K to 860 K.

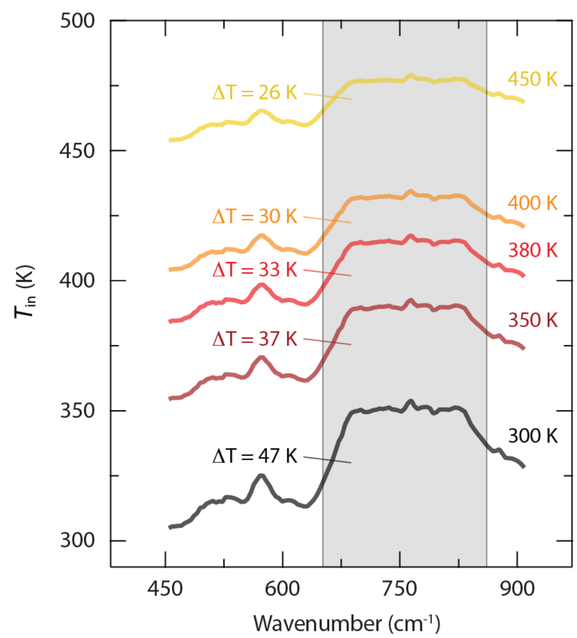

Figure S6 *In-situ* temperature of YAG:3%Ce^{3+} (T_{in}) upon IR excitation in the range of 460–900 cm^{-1} and an applied temperature of 300 K, 350 K, 380 K, 400 K or 450 K, estimated from thermal simulations (see the Methods section). The most effective IR excitation, estimated from the IR absorbance spectrum of YAG:3%Ce^{3+} and total energy of the IR irradiation [Figure 8(a) *bottom*], ranges between 650 cm^{-1} and 860 cm^{-1}, as highlighted by the grey shaded area. Temperature increment due to the IR excitation, averaged over the range of 650–860 cm^{-1}, which is denoted as ΔT, is shown in the figure.

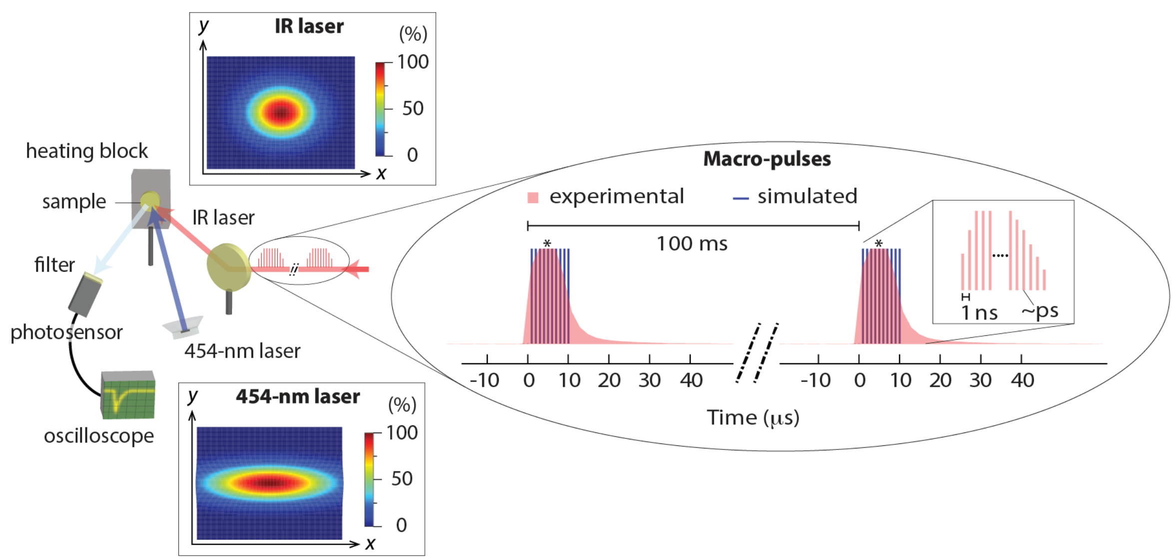

Figure S7 Experimental setup for mode-selective vibrational excitation measurements performed at the FELIX facility. Experimental details, involving simulated energy distributions (*xy*-plane) of the 454-nm laser beam [FWHM = 2 mm (*x*-direction) and = 0.7 mm (*y*-direction)] and IR laser beam [FWHM = 1 mm (*x*- and *y*-directions)], and pulse structure of the IR laser are shown in respective close-up views. Here, the IR laser beam comprises marco-pulses separated by 100 ms and each marco-pulse comprises a number of micro-pulses with a repetition frequency of 1 GHz, *i.e.* with a separation of 1 ns.

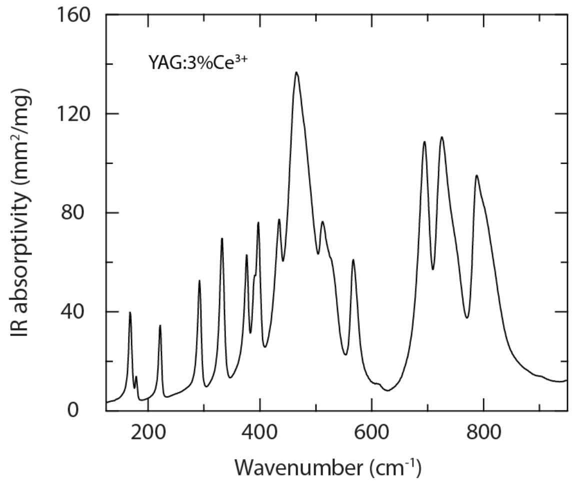

Figure S8 IR absorptivity of YAG:3%Ce^{3+} in the range of 125–950 cm^{-1}. The figure is adapted from ref. S1 (Copyright 2018 American Chemical Society).

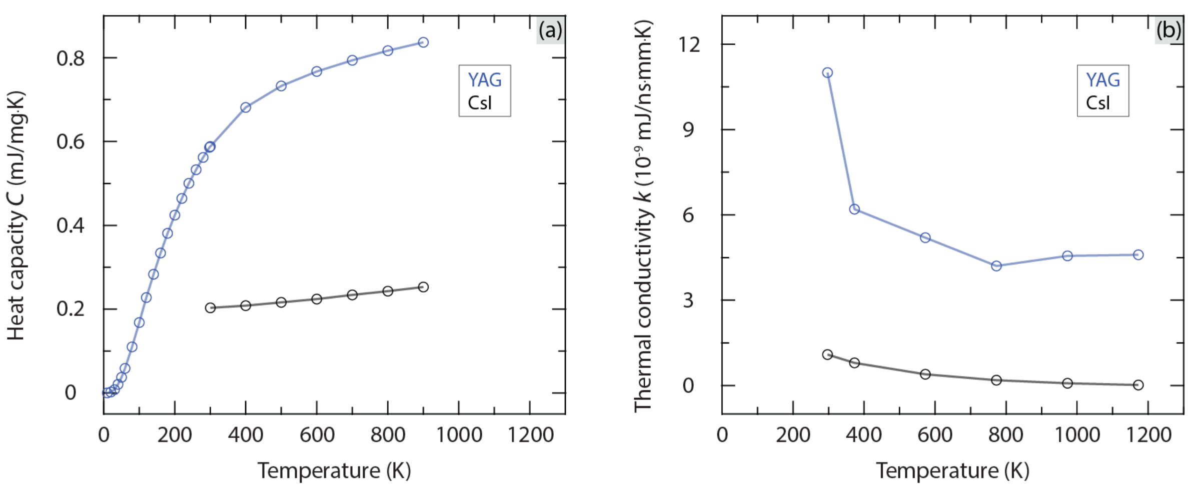

Figure S9 (a) Heat capacity (C) and (b) thermal conductivity (k) of YAG and CsI as a function of temperature, adapted from refs. S2 (Copyright 1998 Elsevier), S3 (Copyright 2014 Elsevier), S4 (Copyright 2014 The American Ceramic Society), and S5 (Copyright 1982 IOP Publishing). For the thermal simulations (see the Methods section), the thermal properties of YAG shown here were assumed to be the same as that of YAG:Ce^{3+}.

References

(S1) Y.-C. Lin, P. Erhart, M. Bettinelli, N. C. George, S. F. Parker and M. Karlsson, *Chem. Mater.*, 2018, **30**, 1865–1877.

(S2) R. J. M. Konings, R. R. Van der Laan, A. C. G. Van Genderen and J. C. Van Miltenburg, *Thermochim. Acta*, 1998, **313**, 201–206.

(S3) F.-Z. Roki, M.-N. Ohnet, S. Fillet, C. Chatillon and I. Nuta, *J. Chem. Thermodyn.*, 2014, **70**, 46–72.

(S4) J. Hostaša, J. Matějíček, B. Nait-Ali, D. S. Smith, W. Pabst and L. Esposito, *J. Am. Ceram. Soc.*, 2014, **97**, 2602–2606.

(S5) D. Gerlich and P. Andersson, *J. Phys. C: Solid State Phys.*, 1982, **15**, 5211–5222.